CARBON AS NEGATIVE ELECTRODES IN LITHIUM SECONDARY CELLS

R. KANNO*, Y. TAKEDA, T. ICHIKAWA, K. NAKANISHI and O. YAMAMOTO
Department of Chemistry, Faculty of Engineering, Mie University, Tsu 514 (Japan)

Summary

The charge and discharge behaviors of lithium cells with carbon electrodes have been examined in 1 M $LiClO_4$ in PC/DME electrolyte. The thermal decomposition products of poly(2-chloro-1-phenylacetylene) and the carbon fiber M46 showed a high anode performance in lithium secondary cells. The lithium storage mechanism was examined by XPS and X-ray diffraction measurements. The intercalated lithium ions participate mainly in the highly reversible cell reaction.

1. Introduction

During the past decade, substantial research effort has been directed into the development of rechargeable lithium batteries. Although some improvements in cycle life and efficiency have been achieved, the reversibility of the lithium electrode remains as a significant problem in aprotic solvent-based electrolytes. The major problems limiting cycle life are short circuits resulting from the growth of lithium dendrites, and macroscopic shape changes during the recharge process. One solution to these problems is to use a lithium–aluminum alloy instead of pure lithium [1, 2]; β-LiAl electrodes restrain the formation of dendrites and therefore exhibit good rechargeability. Unsatisfactory mechanical stability is evident, however, due to the large volume change caused by the phase transformation that occurs during the removal or addition of lithium [3]. The other approach is to select the electrolyte solution [4]. However, complex and costly methods of solvent and electrolyte purification are necessary to obtain high efficiencies. Recently, the thermal decomposition products of polymers such as poly(phenylene) and poly(alylacetylene) have been reported as having a capability as negative electrodes in lithium cells [5, 6]. The lithium–carbon anode might be an attractive alternative for use in secondary lithium batteries if long cycle life is achieved. However, no details of these electrodes have been reported. The present paper is concerned with cycling studies on various carbon anodes using not only the thermal decomposition product of

*Author to whom correspondence should be addressed.

0378-7753/89/$3.50

polymers but also carbon fibers. We found that carbon fiber also showed a high rechargeability efficiency. In addition, the electrode reaction mechanisms of both carbon fiber and the thermal decomposition products of polymers has been examined in detail.

2. Experimental

Carbon fiber and the thermal decomposition products of polymers were used for the electrode materials: polymers were heated at 400 °C for 2 h and then at 800 °C for 2.5 h under a pure nitrogen gas flow. The cells used for the electrochemical tests were cylindrical. The working electrode consisted of a mixture of 50 mg of carbon and 5 mg of Teflon powder pressed into a 13 mm dia. tablet under a pressure of 9 MPa. The counter electrode was a disk of lithium metal foil 15 mm in dia. The separator was a microporous poly(propylene) sheet. The electrolyte was 1 M $LiClO_4$ in 1:1 propylene carbonate–1,2-dimethoxyethane by weight. X-ray photoelectron spectroscopy (XPS) spectra were measured with a Shimazu ESCA 750 spectrometer. X-ray powder diffraction (XRD) data were collected under Ar with Cu Kα radiation using a high power X-ray diffractometer (Rigaku RAD 12kW) equipped with a graphite monochromater.

3. Results and discussion

Lithium storage capacity

Table 1 shows the thermal decomposition products and the carbon fiber examined in this study together with the resistivity and specific surface areas measured by the BET method. Figure 1 shows the first and fifth cycle storage capacities of the electrodes, using the thermal decomposition products of polymers, as a function of the specific surface area. The current density was 0.35 mA cm^{-2}, and the cut-off voltages were −0.03 V for charge and 2.5 V for discharge. Only a portion of the lithium stored at the first charge process was removed by the discharge cycle and the efficiency decreased rapidly with cycling. The storage capacities of the thermal decomposition products, other than that of PPCA, decreased with surface area, both at the 1st and the 5th cycle, indicating that lithium storage is explained by charging the double layers on the thermal decomposition carbon electrodes. The storage capacities of the decomposition product of PPCA, on the other hand, did not decrease significantly after the 2nd cycle: cycling efficiency at the 5th cycle was calculated to be more than 90%, based on the amount of storage at the 2nd cycle. This suggests an electrode reaction mechanism different from those of the other polymer thermal decomposition products.

The surface areas and the relative resistivities of the thermal decomposition products of PPCA at various temperatures are shown in Table 2. The

TABLE 1

Surface areas and relative resistivities of thermal decomposition products of polymers and carbon fibers

	Polymer or carbon fiber	Surface area ($m^2 g^{-1}$)	Relative resistivity
Thermal decomposition products of polymers	PPCA	430	447
	PVDF	880	1081
	PVDC	510	764
	POB	280	49
	PS	100	64300
	PEPY	6	53090
	PVC	4	764
	Graphite	4	1
Carbon	M46	1.3	54.6
	T300 (Toray Industries, Inc.)	1.6	317
	GM60019	1.3	72.8
	GM6060ST (Toa Nenryo Kogyo, kk.)	0.7	190.5
	GF8 (Nippon Carbon Co. Ltd.)	0.4	237
	A6000 (Asahi Nippon Carbon Co. Ltd.)	4.9	
	HTA-7	3.6	
	BP1034AES (Toho Rayon Co. Ltd.)	1.1	79.8

PVDF: Poly(vinylidenefluoride)
PVDC: Poly(vinylidenechloride)
POB: Polyoxybenzoate
PS: Polysulfone
PEPY: Polyetherpolyimide
PVC: Poly(vinylchloride)
PPCA: Poly(2-chloro-1-phenylacetylene)

TABLE 2

Surface areas and relative resistivities, at various temperatures, for PPCA thermal decomposition products

Decomposition temperature (°C)	Surface area ($m^2 g^{-1}$)	Relative resistivity
600	310	1×10^6
800	430	450
1000	210	140
1200	120	120

relative resistivity decreases with decomposition temperature and the specific surface area showed a maximum value of 430 $m^2 g^{-1}$ at a decomposition temperature of 800 °C. Figure 2 shows the fifth cycle storage capacities of

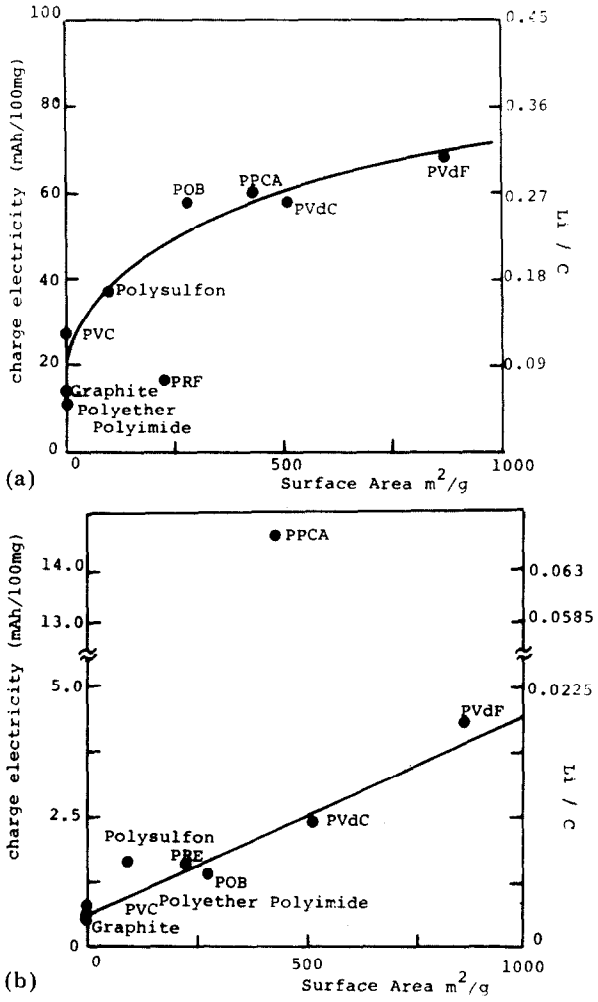

Fig. 1. Surface area dependence of the lithium storage capacity at 1st (a) and 5th (b) charge–discharge cycles for the polymer electrodes decomposition product.

the electrodes, using the thermal decomposition products of PPAC, as a function of surface area. The thermal decomposition product of PPCA at 800 °C, which has the largest surface area, showed the highest lithium storage capacity, indicating that the surface of the PPCA decomposition product participates strongly in the highly reversible storage of lithium, and that the resistivity of the decomposition product does not influence the storage capacity.

Figure 3 shows the first and fifth cycle storage capacities of carbon fiber electrodes as a function of the specific surface area. The storage capacity decreases with surface area at the 1st cycle, whereas at the 5th cycle, the capacity other than for M46, did not change significantly with surface area. This indicates that reversible lithium storage does not proceed by a

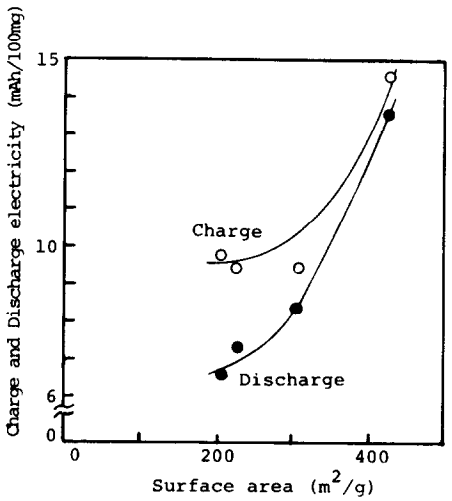

Fig. 2. Surface area dependence of the discharge and charge capacities at the 5th cycle, prepared at various temperatures for the PPAC decomposition products electrode.

surface reaction on the carbon fiber alone. Furthermore, the high cycling efficiency of the M46 carbon fiber suggests an electrode reaction mechanism different from that of the other carbon fibers.

OCV and cycling properties

Figure 4 shows the open circuit voltage (OCV) of the Li/carbon cell at room temperature as a function of stored lithium on the carbon electrodes. The OCV of the carbon fiber decreases slowly from 0.8 V at a lithium storage level of 0.014 Li/C to 0 V at 0.09 Li/C after a rapid decrease with discharge around 0 Li/C. The thermal decomposition products of PPCA, on the other hand, show OCV curves different from those of the M46 carbon fiber electrodes; the OCV is slightly higher than that of the carbon fiber in a shallow lithiated range; furthermore the curves show decomposition temperature dependence.

To understand the details of the lithium storage process, we examined the cycling behavior of the Li/carbon cell at different lithium storage levels with a charge and discharge depth of 0.004 Li/C. The current density was 0.5 A cm^{-2}. The cell with PPCA thermal decomposition products only showed good rechargeability within the narrow range 0.157 - 0.161 Li/C, whereas in both shallower and deeper ranges, the rechargeability was extremely poor. For the carbon fiber cell, the highest rechargeability efficiency was obtained at a lithium storage level of 0.1125 Li/C, as shown in Fig. 5.

XPS data

The XPS spectra of the lithium 1s 1/2 state and the carbon 1s 1/2 state were measured at various lithium storage levels. The XPS data on the thermal decomposition products of PPCA are shown in Fig. 6. In the shallow li-

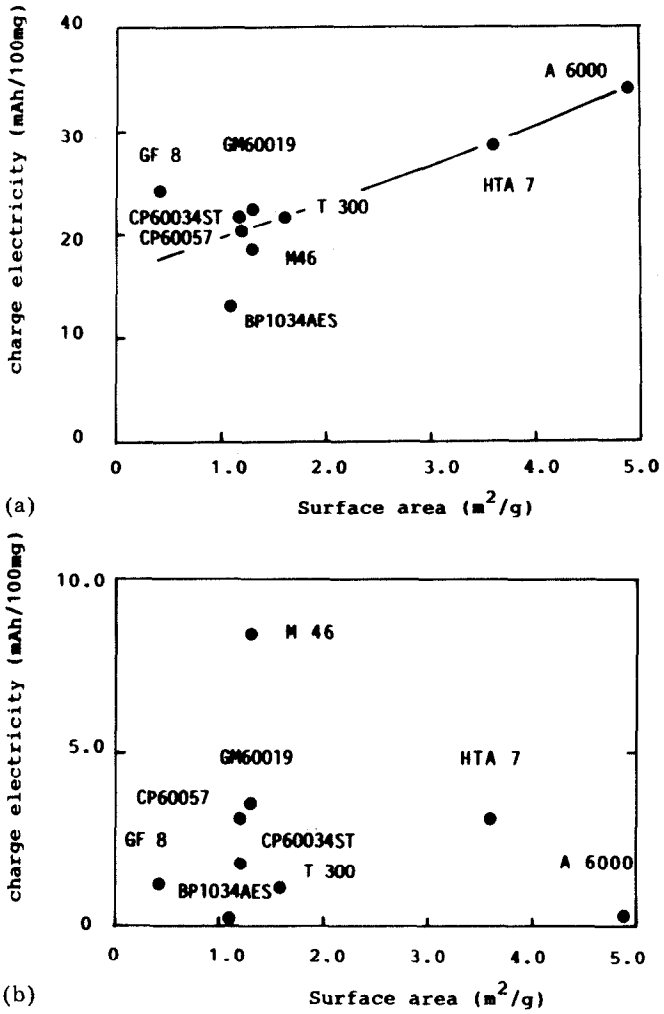

Fig. 3. Surface area dependence of the lithium storage capacity at tne 1st (a) and 5th (b) charge–discharge cycle for the carbon fiber electrodes.

thiated region of 0.04 Li/C, the chemical shift of the Li 1s 1/2 peak (E = 54.89 eV), which is close to that of metallic lithium (E = 54.69 eV), may be due to absorbed lithium atoms forming the electric double layer on the carbon surface. The peak, however, shifts to higher energy with lithiation, and the chemical shift (E = 55.49 eV) at the lithiated region around 0.21 Li/C, where the Li/PPCA couple showed the highest rechargeability efficiency, may correspond to a different absorbed state of lithium.

The decomposition product of PPCA showed carbon 1s 1/2 spectra at E = 284.4 eV. The C 1s 1/2 spectra for the lithiated PPCA electrode also showed a new peak which has a higher binding energy (E = 285.7 eV) than the C 1s peak observed for the non-lithiated sample (E = 284.4 eV). The

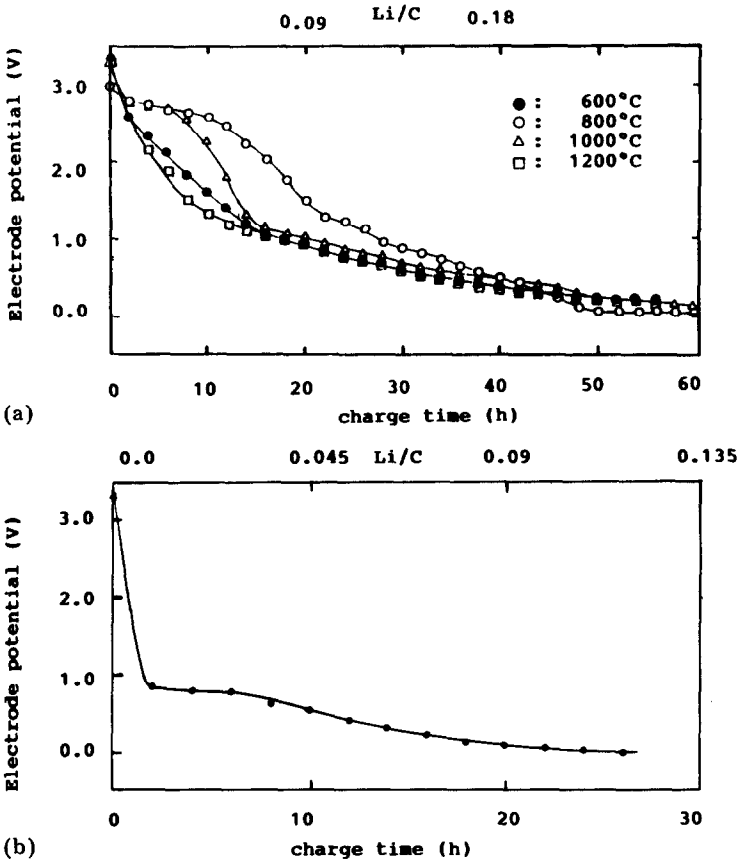

Fig. 4. Open circuit voltage (OCV) curves of the carbon electrodes. (a) OCV curves, prepared at different temperatures, of the PPCA thermal decomposition product electrodes, (b) OCV curve of the carbon fiber (M46) electrode.

peak height of the new peak increases with lithiation to a maximum around 0.21 Li/C, where the Li/decomposition product of the PPCA couple showed the highest rechargeability efficiency.

The XPS data on the carbon fiber [7] suggest the same electrode reaction mechanism to that obtained for the PPCA decomposition products, described above. The chemical shift of the Li 1s 1/2 peak (E = 54.80 eV) at 0.022 Li/C shifts to a higher energy with lithiation, and the chemical shift (E = 55.12 eV) at 0.09 Li/C, where the Li/M46 fiber couple showed a high rechargeability efficiency, may correspond to a different lithium ions state. In a deeper lithiated range of 0.22 Li/C, the Li 1s peak again shifts to lower energy, suggesting lithium metal deposition on the surface of the carbon fiber.

XRD measurements

Figure 7 shows the XRD pattern of the carbon fiber electrodes at various lithiation levels. The XRD peak around d = 3.5 Å, which was indexed

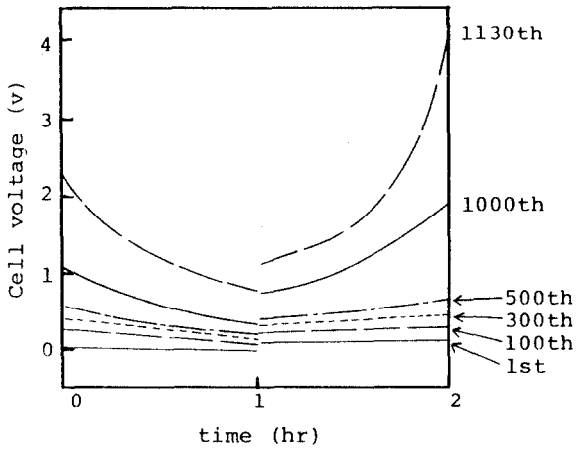

Fig. 5. Cycling behavior of an Li/M46 cell at a lithium storage level of 0.1125 Li/C (25 mA h 100 mg^{-1}). The current density was 500 A cm^{-2}.

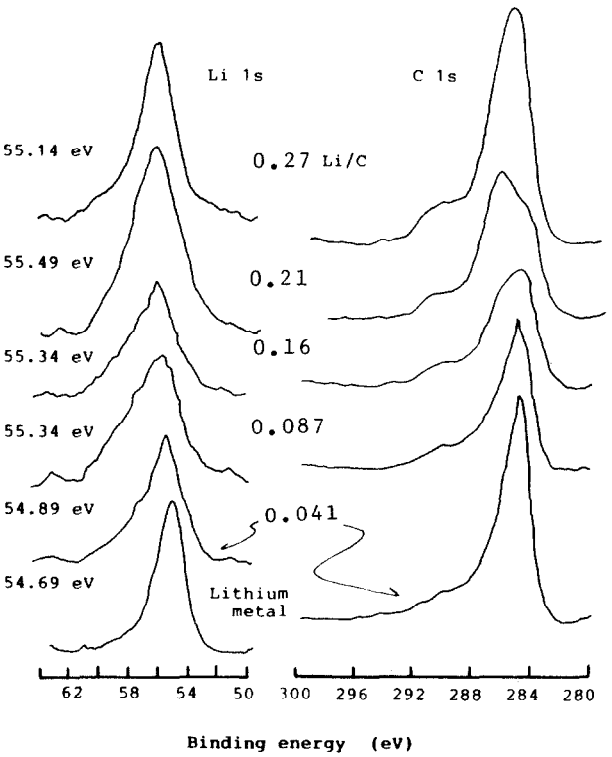

Fig. 6. XPS spectra of the thermal decomposition products of PPCA at a different lithium storage level.

as (002), shifts to a higher d-value, from 0 to 0.13 Li/C. The c-axis parameter calculated from the XRD data increases with lithiation from 6.85 Å at 0 Li/C to 7.08 Å at 0.13 Li/C, indicating that the lithiation proceeds by an

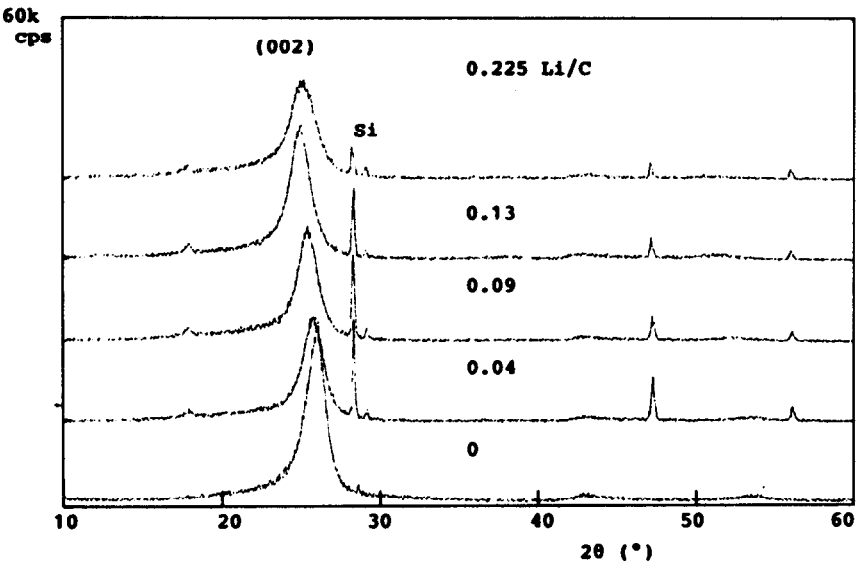

Fig. 7. XRD pattern of the M46 carbon fiber electrode at a different lithium storage level.

intercalation of lithium or solvated lithium ions into the carbon layer. The XRD peak did not shift above 0.13 Li/C, suggesting that lithium begins to deposit on the surface of the carbon fiber. The XR data obtained here are consistent with the XPS data described above.

Lithium intercalation into the electrode could not be confirmed by XRD data for the PPCA thermal decomposition products because the XRD peaks were too broad to calculate their *d*-values. A similar change of binding energy in the PPCA thermal decomposition products suggests, however, the same reaction mechanism as that explained for the lithiation of the carbon fiber electrodes.

References

1 A. N. Dey, *J. Electrochem. Soc., 118* (1971) 1547.
2 I. Epelboin, M. Forment, M. Garreau, J. Thevenin and D. Warin, *J. Electrochem. Soc., 127* (1980) 2100.
3 J. Rene van Beek and P. J. Rommers, in J. Thompson (ed.), *Power Sources 7*, Academic Press, London, 1979, p. 595.
4 J. L. Goldman, R. M. Mank, J. H. Young and V. R. Koch, *J. Electrochem. Soc., 127* (1980) 1461.
5 H. Hayashi and T. Fujii, *Japan Pat. 154763* (1984).
6 M. Miyabayashi and A. Itsubo, *Japan Pat. 147456* (1986).
7 R. Kanno, Y. Takeda, T. Ichikawa, F. Kohno and O. Yamamoto, to be published.